Journal of Alloys and Compounds 506 (2010) 279–284

Contents lists available at ScienceDirect

Journal of Alloys and Compounds

journal homepage: www.elsevier.com/locate/jallcom

Structural and magnetic properties of $Cu_xMg_{0.5-x}Zn_{0.5}Fe_2O_4$ ($x = 0$–0.5) particles

Azadeh Ashrafizadeh[a,*], Ali Ghasemi[a,b], Andrea Paesano Jr.[c], Carla Fabiana Cerqueira Machado[c], Xiaoxi Liu[a], Akimitsu Morisako[a]

[a] Spin Device Technology Center, Faculty of Engineering, Shinshu University, Nagano, Japan
[b] Department of Materials Engineering, Malek Ashtar University of Technology, Shahin Shahr, Iran
[c] Centro de Ciências Exatas, Departamento de Física, Universidade Estadual de Maringá, Brazil

ARTICLE INFO

Article history:
Received 27 April 2010
Received in revised form 29 June 2010
Accepted 30 June 2010
Available online 7 July 2010

Keywords:
Ferrite
Magnetic properties

ABSTRACT

The $Cu_xMg_{0.5-x}Zn_{0.5}Fe_2O_4$ ($x = 0$, 0.1, 0.2, 0.3, 0.4 and 0.5) ferrites were prepared by sol–gel method. The effect of copper content on the structural and magnetic properties was investigated by X-ray diffraction (XRD), Mössbauer spectroscopy (MS), field emission scanning electron microscopy (FESEM), transmission electron microscopy (TEM), vibrating sample magnetometer (VSM) and magnetic susceptometer. Results show that single spinel ferrite particles were prepared by controlling the type and amount of additive. Copper content has significant influence on magnetic properties of prepared samples. It was found that with increasing copper in $Cu_xMg_{0.5-x}Zn_{0.5}Fe_2O_4$, saturation magnetizations along with grain size were increased while the values of coercivity were decreased. The variation of effective magnetic susceptibility exhibits almost linear trend with magnetic field. A frequency-dependence peak was observed in ac magnetic susceptibility versus temperature for fine particles which is well fitted by Vogel–Fulcher model. It was proved that there is strong magnetic interaction among prepared nanoparticles.

1. Introduction

Soft magnetic materials have great potential application in electronic industry. The most common type is cubic spinel ferrites with formula AB_2O_4 which contains tetrahedral (A site) and octahedral (B site) crystalline sites. The magnetic and electrical properties of soft ferrite could be easily tuned by incorporation and suitable distribution of additional cations (divalent or trivalent) in the spinel structure. Mg–Zn ferrite has cubic spinel structure and is widely used in many electronic devices because of high electrical resistivity, hard mechanical properties, high Curie temperature and environmental stability [1,2]. The sintering temperature of Mg–Zn ferrite is relatively high (more than 1300 °C) which is the main drawback for utilizing these materials in some applications. By partial substitution of Mg with Cu, it is realized that the sintering temperature could be reduced [1,3]. At high sintering temperature the role of CuO as a sintering aid is to form liquid phase among grain boundaries and consequently to cause grain growth and enhancement of density. It is found that with diffusion of copper cations into crystal structure of Mg–Zn ferrite during sintering process, the magnetic properties coupled with dielectric characteristics will not deteriorated [3,4]. Several investigators have studied the magnetic and electrical properties of Mg–Zn ferrites by partially substituting Mg with Cu ions to be fabricated by different methods [4–8]. However there is still some lack in magnetic characteristics of this type ferrite, particularly magnetic susceptibility of Mg–Cu–Zn ferrite is not widely studied. With this view in mind the present paper premise deals with the formation and magnetic properties of $Cu_xMg_{0.5-x}Zn_{0.5}Fe_2O_4$ ($x = 0$, 0.1, 0.2, 0.3, 0.4 and 0.5) in powder configuration in micron and nanosize range by sol–gel method. The magnetic susceptibility versus applied field and temperature was investigated for Mg–Cu–Zn ferrite respectively. The role of copper cations on the saturation magnetization, coercivity, grain growth and phase formation of Mg–Zn ferrite is also evaluated.

2. Experimental

The Mg–Cu–Zn ferrites with composition of $Cu_xMg_{0.5-x}Zn_{0.5}Fe_2O_4$ (x varies from 0 to 0.5 with step of 0.1) with particle size of 100 nm to 2 μm and less than 30 nm were prepared by controlling the amount of additives introduced in the sol–gel method. The aqueous sol was produced by dissolving iron nitrate, copper nitrate, magnesium nitrate and zinc nitrate, according to desired stoichiometric proportion, in deionized water and then mixed together by constant stirring. Citric acid was added to the sol for the enhancement of nitrates dissolution. The pH value of solution was adjusted to 7 using ammonia. All of the solutions were dark brown indicating, the presence of Fe^{3+} ions. The gels were obtained by slow evaporation at 70 °C until gel dried. The powders were sintered at 1000 °C for 2 h. The nanoparticles were employed to investigate the variation of blocking temperature with frequency. The phase identification of the powders was carried out by an X-ray diffractometer (XRD) with CuK_α radiation. The MS characterizations were performed in the transmission geometry, using a conventional spectrometer, operated in the constant acceleration mode. The γ-rays were provided by a 57Co(Rh) source, with a nominal starting activity of 25 mCi. The Mössbauer spectra were analyzed using a non-linear least-square routine, with lorentzian line shapes. Eventually, a hyperfine magnetic field distribution, B_{hf} Dist., was used as histograms in the spectral analysis. All isomer shift (δ) data are given relative to α-Fe throughout this paper. The

* Corresponding author. Tel.: +81 26 269 5481; fax: +81 26 269 5495.
E-mail address: aza_ashrafi62@yahoo.com (A. Ashrafizadeh).

0925-8388/$ – see front matter © 2010 Elsevier B.V. All rights reserved.
doi:10.1016/j.jallcom.2010.06.191

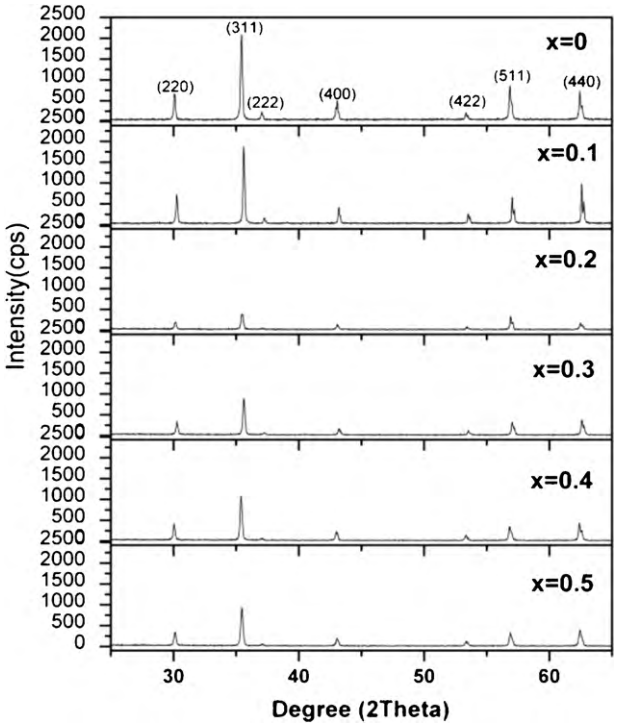

Fig. 1. XRD patterns of $Cu_xMg_{0.5-x}Zn_{0.5}Fe_2O_4$ prepared by sol–gel processing.

morphology and size distribution of nanoparticles were investigated by field emission scanning electron microscopy (FESEM) and transmission electron microscopy (TEM) model JEOL 2010. The magnetic properties were studied by vibrating sample magnetometer (VSM). The ac magnetic susceptibility has been measured versus static magnetic field and temperature at different frequencies in the selected range of 40–1000 Hz and 100–300 K respectively, using a Lake Shore ac susceptometer model 7000.

3. Results and discussion

3.1. Structural and magnetic analysis of micron sized particles

3.1.1. Structural characteristics

The XRD patterns of samples in Fig. 1 revealed that in all samples, by substituting Mg with Cu, no extra peak corresponding to any secondary phases were identified. Based on the XRD results, it seems that copper cations could be rearranged in the spinel structure of Mg–Zn ferrite. It is reasonable to conclude from the patterns that the spinel phases can be formed in the all specimens at relatively low sintering temperature and time. Consequently, copper could play as a suitable sintering aid for fabrication of Mg–Zn ferrite at temperature lower than solid state reaction. It must be noted that the nature of sol–gel process is to reduce the final sintering temperature and this obvious reduction of sintering temperature can be attributed to the utilizing Cu cations coupled with driving force of sol–gel process.

Fig. 2 shows the RT Mössbauer results for some representative samples. The spectra revealed ferrites not completely magnetically ordered and were fitted considering hyperfine magnetic field distributions (see insets, in the figures). Table 1 presents the obtained hyperfine parameters, for the whole series of samples. According to this data, all the iron cations are in the ferric state (Fe^{3+}). Substitution of magnesium by copper from $x = 0.5$ down to $x = 0.2$ does not significantly change the average magnetic hyperfine field. However, a clear decrease occurs from $x = 0.1$, including the appearing of a paramagnetic fraction for the $x = 0$ sample. Earlier results on the copper ($CuFe_2O_4$), magnesium ($MgFe_2O_4$) and zinc ($ZnFe_2O_4$) stoichiometric ferrites have shown that only the

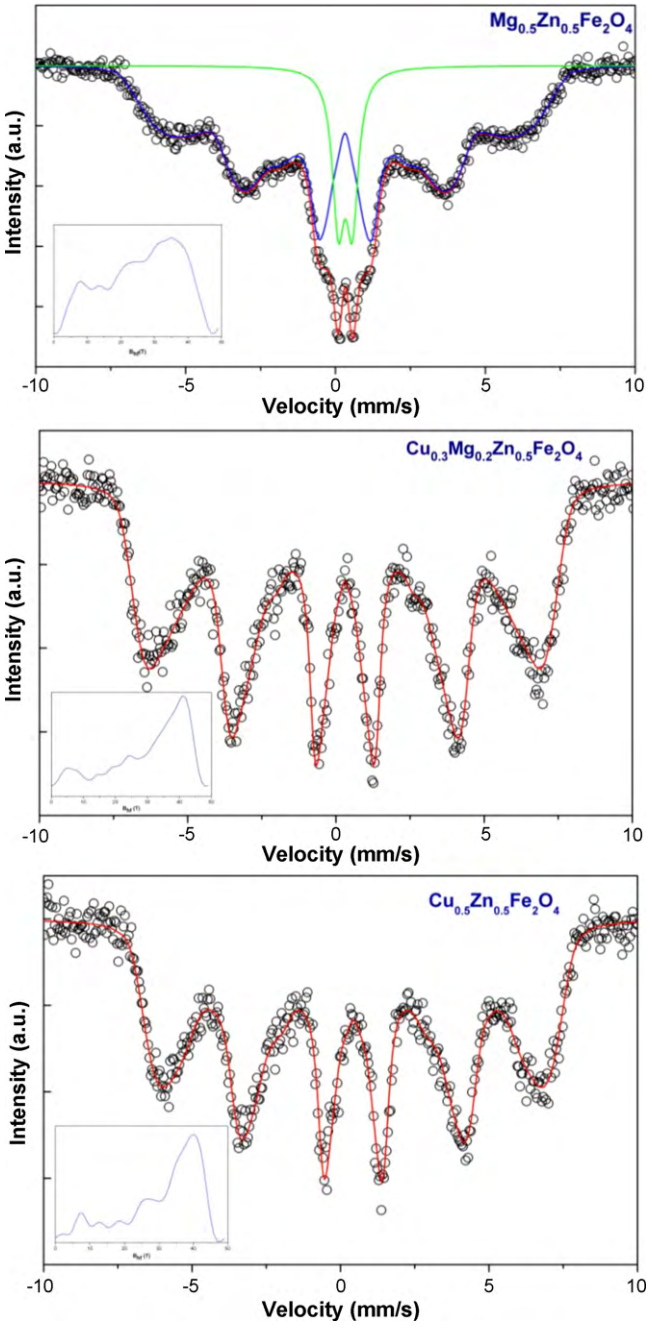

Fig. 2. Mössbauer spectra of $Cu_xMg_{0.5-x}Zn_{0.5}Fe_2O_4$ with $x = 0$, 0.3 and 0.5.

zinc ferrite is not magnetic at RT. Besides, the former is an inverse spinel ($B_{hf} \sim 480$ kOe/site A – 512 kOe/site B), the middle one is a partially inverse spinel (degree of inversion ~0.9; $B_{hf} \sim 482$ kOe/site A – 500 kOe/site B) whereas the later is a normal spinel. Therefore,

Table 1
Hyperfine parameters for the ferrite samples (IS = somer shift; QS = quadrupole splitting; B_{hf} = hyperfine magnetic field; Γ = linewidth).

Sample	Site	IS (mm/s)	QS (mm/s)	B_{hf} (T)	Γ (mm/s)	Area (%)
$x = 0.5$	B_{hf} Dist.	0.31	−0.03	31.0	0.36	100
$x = 0.4$	B_{hf} Dist.	0.30	−0.03	30.7	0.35	100
$x = 0.3$	B_{hf} Dist.	0.30	−0.02	31.9	0.34	100
$x = 0.2$	B_{hf} Dist.	0.30	−0.03	31.6	0.36	100
$x = 0.1$	B_{hf} Dist.	0.29	−0.02	28.9	0.32	100
$x = 0$	B_{hf} Dist.	0.30	−0.03	26.3	0.30	85.8
	Doublet	0.33	0.46	–	0.49	16.2

it is plausible to suppose that for $x = 0$ the trivalent iron is shared nearly half-and-half among the sites A and B, although this is not clearly evidenced in the respective RT spectrum. Then, decreasing the copper content implies in a "migration" of iron cations to the octahedral (B) sites, since part of the magnesium cations go to the tetrahedral (A) sites. As expected, the consequence is the progressive weakening of the hyperfine magnetic field and the appearing of a paramagnetic component (i.e., the doublet) for $x = 0$, from the iron locate at the site B.

Morphology and particle size of synthesized micron sized ferrites were investigated by FESEM. Results show that copper content can act as a contributor on particle size. The increase in particle size with increasing Cu content which is clearly visible in Fig. 3 is according to the prediction.

3.1.2. Magnetic characteristics

Fig. 4a displays narrow hysteresis loops with high saturation magnetization and low coercivity for the synthesized Mg–Cu–Zn ferrites. Fig. 4b illustrated the compositional dependence of saturation magnetization and coercivity. It is revealed that with increasing the amount of copper in the composition, saturation magnetization is increased, while coercive force is decreased. The variations of M_s with chemical composition can be explained on the basis of the exchange interaction between the ions at the tetrahedral (A) and octahedral (B) sites. In the Mg–Cu–Zn ferrite, the stable Zn^{2+} ions occupy only at A sites and Mg^{2+}, Cu^{2+} and Fe^{3+} ions have preference for the B site [1]. The resultant magnetization is difference magnetization between magnetization of A and B sites. By substitution of Mg^{2+} with Cu^{2+} ions, since Cu^{2+} have a magnetic moment of 1 μ_β, magnetization in B site increase and this lead to increase of saturation magnetization.

It is well known that coercivity in polycrystalline ferrites is strongly dependent on the first magnetocrystalline anisotropic constant and grain size. In spinel ferrite the value of first anisotropic constant is small and has no important influence on the coercivity, while in the hexagonal ferrite this parameter could be acted as a very significant contributor. In a polycrystalline sample, the density of the grain boundary is in inverse proportion to the grain size. Accordingly, we conjecture that the pinning of magnetization at the grain boundaries is the most likely cause for determining the coercivity. If the grain size largely increases, however, the coercivity caused by grain boundary pinning will disappear because each grain can be in multi-domain state. Basically, our result is consistent with previous reports, which have shown the fact that the coercivity of ferrite depends on the temperature and the grain size [9,10]. Consequently in this study, it seems that coercivity can be tuned by grain size. Actually, sample $x = 0$ contains the smallest grain size, however sample $x = 0.5$ has the largest size. Since the coercivity has opposite trend with grain size, the coercivity is reduced by an increase in copper content. It is mentioned in the previous section that with increasing copper content, grain size increases, therefore, it can be predicated that coercivity must be reduced by increasing copper amount in the prepared samples. This predication is completely consistent with the obtained results.

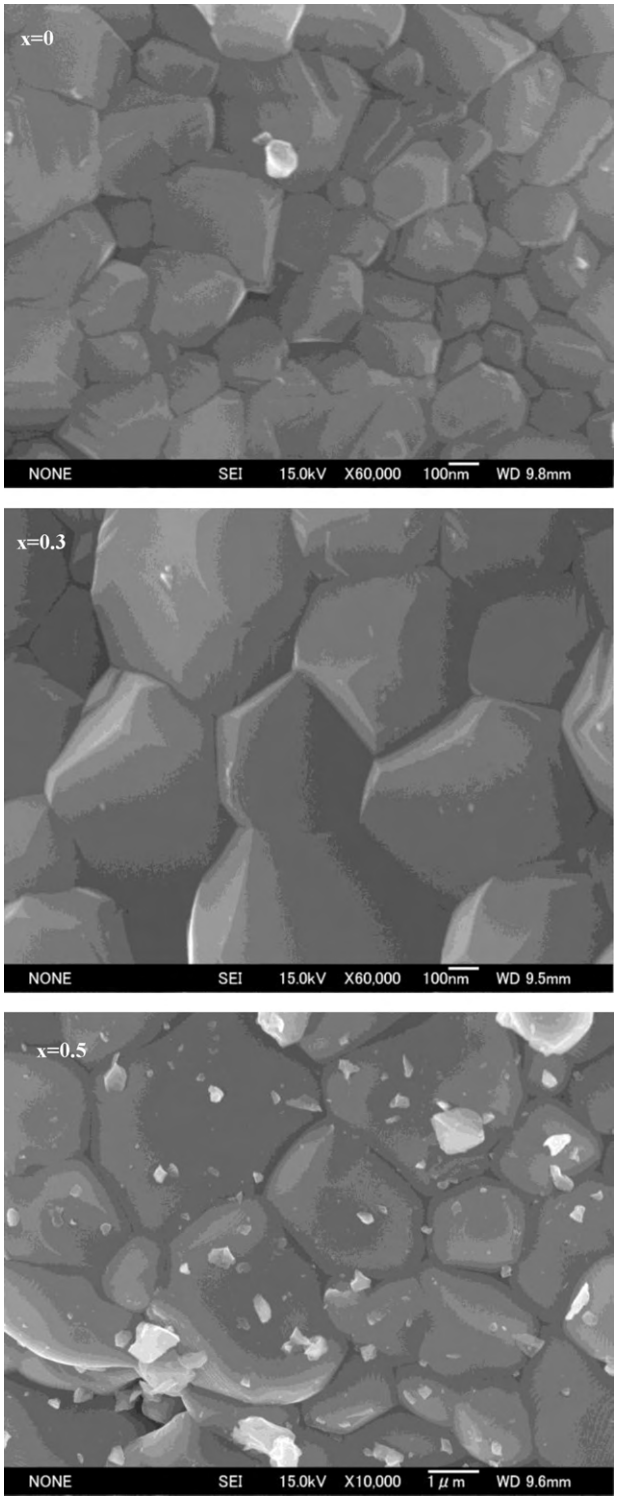

Fig. 3. FESEM micrographs of $Cu_xMg_{0.5-x}Zn_{0.5}Fe_2O_4$ ($x = 0$, 0.3 and 0.5).

3.1.3. Magnetic susceptibility versus static magnetic field

Fig. 5 indicates the variation of effective magnetic susceptibility of micron sized ferrite particles (100 nm to 2 μm) with static magnetic field. It is observed that effective magnetic susceptibility in all samples exhibits linear variation with increasing magnetic field. Based on the experimental findings the mechanism of susceptibility can be proposed as follows: the porosities and inhomogeneity are probably responsible for the domain wall pinning and the observed behavior in effective magnetic susceptibility. If there were no pinning centers in the samples, the domain walls would under the influence of external field take an equilibrium position with minimum energy. With pinning centers, domain walls are pinned in different positions and the field exerts a pressure on them tending to shift into equilibrium position. The further away they are from the equilibrium position, the larger the pressure is. However, pinned domain walls can still move within the potential wall of pinning centers. The smaller the pressure by the field, the larger the mobility of domain walls in the potential wall. When a domain wall gets released from a pinning site under the combined influence of the dc field and the ac field, it will jump to a new stable

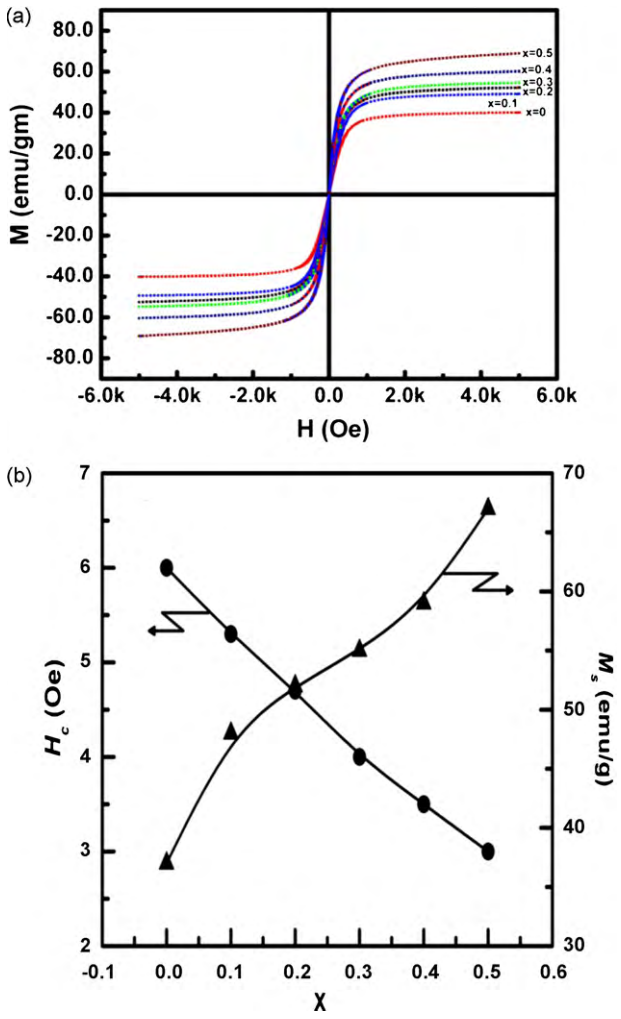

Fig. 4. (a) Hysteresis loops of synthesized Mg–Cu–Zn ferrites; (b) Compositional dependence of coercivity and saturation magnetization.

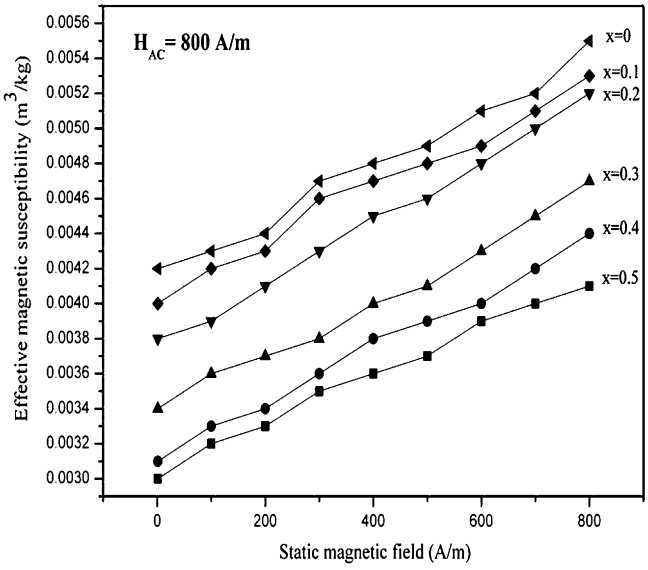

Fig. 5. Variation of effective magnetic susceptibility versus static magnetic field.

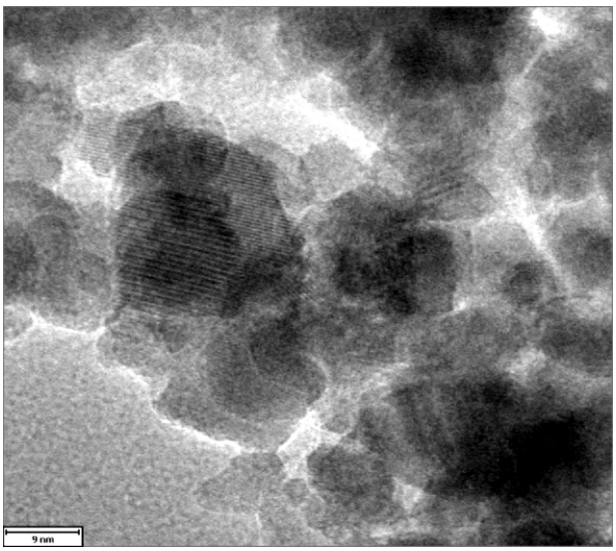

Fig. 6. TEM micrograph of sample with $x = 0.5$.

position. In the new position, it will experience a smaller pressure due to the dc field than in the old position, resulting in an increased mobility of the domain wall in the new position. Jumping back to old sites will not occur because the pressure on the domain walls due to the dc or ac field pushes them in one direction only. After the jump, the domain walls only oscillate in new potential walls, which is a reversible process. They do not have enough energy to jump continuously between the pinning sites.

3.2. Magnetic properties of nanoparticles

The particle size distribution was estimated based on analyzing the bright field images of randomly selected nanoparticles. It reveals from Fig. 6 that the mean particle size is 12 nm. This size is obtained by counting 50 single nanoparticle at various micrographs.

To study the magnetic dynamic behavior of the nanoparticles, the ac magnetic susceptibility of prepared ferrites versus temperature at different frequencies was measured. Fig. 7a and b reflects the temperature dependence of ac magnetic susceptibility at different frequencies in the range of 111–1000 Hz and at an ac magnetic field of 800 A/m for ferrite nanoparticles with composition of $x = 0.5$. It is revealed that imaginary parts exhibit a peak near 270 K which is frequency dependent and shifted to higher temperature with increasing frequency. This characteristic maximum is the signature of blocking/freezing process of the superparamagnetic/spin glass systems [11–15]. The blocking temperature is the threshold point of thermal activation. Above T_B, magnetocrystalline anisotropy is overcome by thermal activation and the magnetization direction of each nanoparticle simply follows the applied field direction. Consequently, the nanoparticles show paramagnetic properties. Below the blocking temperature, thermal activation is no longer able to overcome the magnetocrystalline anisotropy of the nanoparticles. As a consequence, the magnetization direction of each nanoparticle rotates from the field direction back to its own easy axis without any movement of the nanoparticle. Since the nanoparticles and consequently their easy axes are randomly orientated, overall susceptibility is reduced with decreasing temperature as Fig. 7a and b shows.

The interacting or non-interacting behavior of the fine powders was evaluated by Neél–Brown (non-interacting model) and Vogel–Fulcher (interacting law) [16–18]. According to the Neél–Brown model, the blocking temperature measured at a

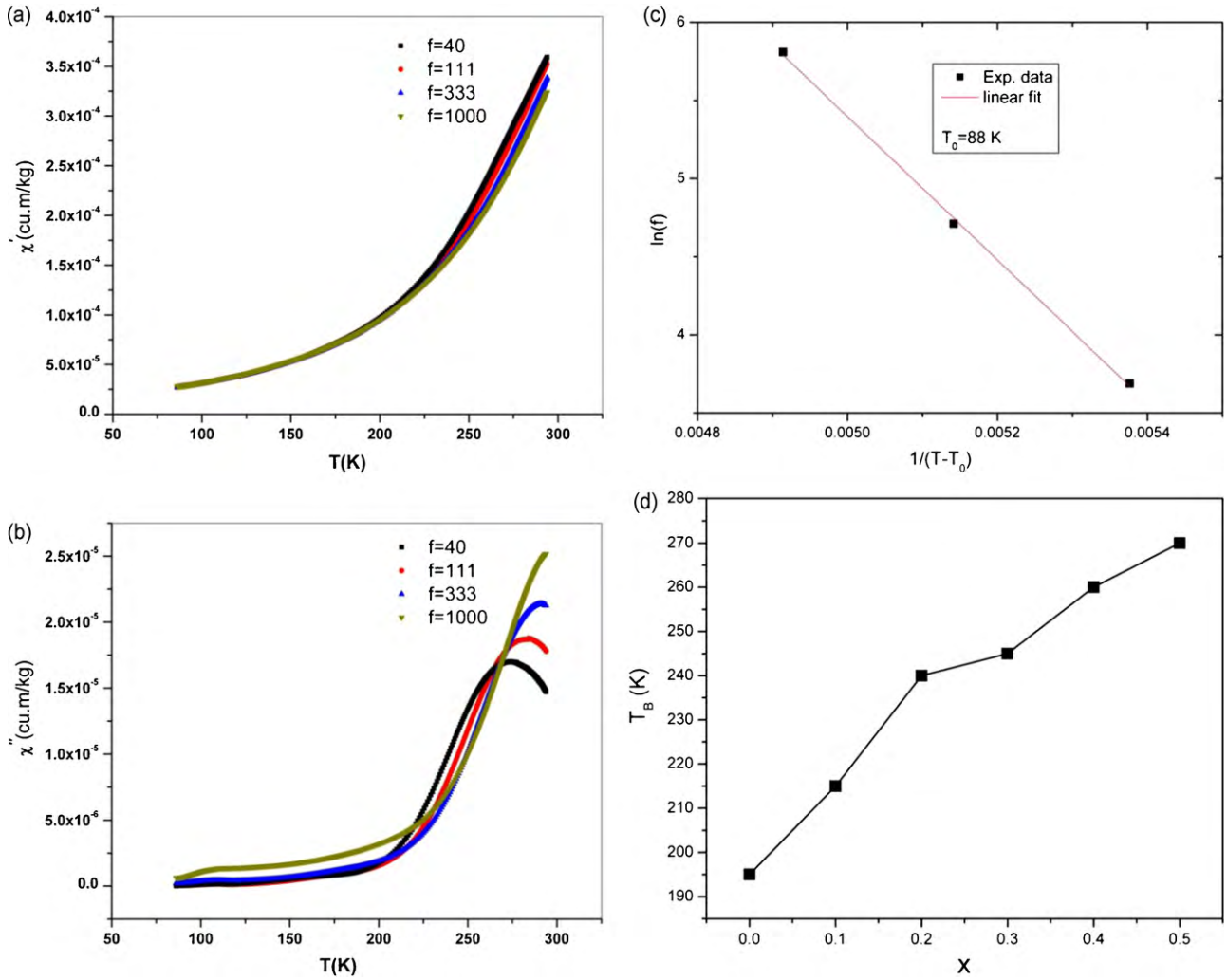

Fig. 7. Real parts (a) and imaginary parts of susceptibility (b) $\ln(f)$ versus $1/(T-T_0)$ (c), blocking temperature versus composition (d).

given working frequency, is related to the considered frequency as: $\ln 1/2\pi\nu = \ln\tau_0 + KV/k_BT_B$. Attempt time is calculated from the curves and it is found that it spreads between τ_0 10^{-27} to10^{-25} s for samples with $x = 0.5$ and $x = 0$ respectively. These values, however, are unphysical, being several orders of magnitude lower than the typical value found in the literature for a non-interacting assembly of superparamagnetic nanoparticles (10^{-8}–10^{-11} s). This suggests that the Neél–Brown model is not appropriate to describe the dynamic behavior of our system. In this case, deviations from the model can be ascribed to the presence on strong interactions, as indeed suggested by TEM image (inset of Fig. 7a) that showed the presence of several large aggregates.

For interacting magnetic nanoparticles, the frequency dependence of T_B is given by the Vogel–Fulcher law [19]:

$$\frac{\ln\ 1}{2\pi\nu} = \ln\tau_0 + \frac{E_a}{k_B(T-T_0)} \quad (1)$$

here E_a is the energy of barrier, T_0 is an effective temperature which reveals the existence of the interaction between nanoparticles and T is the characteristic temperature indicating the onset of the blocking process. We tried to fit the experimental data of $\chi''(T)$ for our samples, using Eq. (1). By fitting the experimental data from ac magnetic susceptibility (Fig. 7c) it was found that the value of attempt time is 5×10^{-12} s. Since the maximum of susceptibility is at a temperature higher that 200 K, it is likely because of the interparticle interactions a pure superparamagnetic (SP) regime is not attained at room temperature. This would be coherent with the fact that coercivity and remanence are almost zero in our samples and not exactly zero, as expected for a pure SP. The interaction between nanoparticles affected the blocking/freezing temperature by modifying the potential barrier. By increasing the strength of interaction, T_B shifts to higher temperatures.

In Fig. 7d, we see that the blocking temperature increases almost linearly with increasing Cu concentration in the samples. The main reason is attributed to the size of nanoparticles. Basically, with increasing Mg content and hence reducing Cu content in the composition the size and distributions of particles are decreased. It is well known that blocking temperature has linear proportional to the volume of particles and anisotropy constant. Consequently, it is reasonable to have the mentioned trend in blocking temperature versus copper content. Another contributor which must also be considered is the amount of paramagnetic phases in the prepared samples. It was clarified by MS results that the amount of paramagnetic phase is increased by reducing copper content. Therefore the anisotropy constant is higher for copper rich samples compared with the Mg rich ferrites.

4. Conclusions

The Mg–Cu–Zn ferrites with composition of $Cu_xMg_{0.5-x}Zn_{0.5}Fe_2O_4$ were prepared in powder configuration by sol–gel method. Substitution of magnesium by copper from

$x = 0.5$ down to $x = 0.2$ does not significantly change the average magnetic hyperfine field. However, a clear decrease occurs from $x = 0.1$, including the appearing of a paramagnetic fraction for the $x = 0$ sample. Saturation magnetization increases with increasing of copper content. Coercive force was decreased by adding copper ions and effective magnetic susceptibility was increased by increasing of copper concentration. It is observed that effective magnetic susceptibility in all samples exhibits linear variation with increasing magnetic field. The good agreement between experimental data of magnetic susceptibility and Vogel–Fulcher model confirms the existence of strong interactions between nanoparticles.

Acknowledgements

This work was supported in part by Grant-in-Aid for JSPS Fellows from Japan Society for Promotion of Science (JSPS) and Grants-in-Aid for Scientific Research (B).

References

[1] M. Manjurul Haque, M. Huq, M.A. Hakim, Mater. Chem. Phys. 112 (2008) 580–586.
[2] E. Rezlescu, N. Rezlescu, P.D. Popa, L. Rezlescu, C. Pasnicu, M.L. Craus, Mater. Res. Bull. 33 (1998) 915–925.
[3] M. Manjurul Haque, M. Huq, M.A. Hakim, J. Magn. Magn. Mater. 320 (2008) 2792–2799.
[4] N. Rezlescu, E. Rezlescu, P.D. Popa, M.L. Craus, L. Rezlescu, J. Magn. Magn. Mater. 182 (1998) 199–206.
[5] S.R. Murthy, Bull. Mater. Sci. 24 (2001) 379–383.
[6] A. Verma, T.C. Goel, R.G. Mendiratta, P. Kishan, J. Magn. Magn. Mater. 208 (2000) 13–19.
[7] Z. Yue, J. Zhou, L. Li, X. Wang, Z. Gui, Mater. Sci. Eng. B 86 (2001) 64–69.
[8] Z. Yue, J. Zhou, X. Wang, Z. Gui, L. Li, J. Mater. Sci. Lett. 20 (2001) 1327–1329.
[9] A. Ghasemi, A. Morisako, J. Alloy Compd. 456 (2008) 485–491.
[10] A. Ghasemi, A. Hossienpour, A. Morisako, A. Saatchi, M. Salehi, J. Magn. Magn. Mater. 302 (2006) 429–435.
[11] J.L. Dormann, D. Fiorani, D. Tronc, J. Magn. Magn. Mater. 202 (1999) 251–267.
[12] P.E. Jönsson, Adv. Chem. Phys. 128 (2004) 191–248.
[13] M. Suzuki, S.I. Fullem, I.S. Suzuki, Phys. Rev. B 79 (2009) 024418–024425.
[14] D. Parker, V. Dupuis, F. Ladieu, J.P. Bouchaud, E. Dubois, R. Perzynski, E. Vincent, Phys. Rev. B 77 (2008) 104428–104437.
[15] S. Vasseur, E. Duguet, J. Portier, G. Goglio, S. Mornet, E. Hadová, K. Knížek, M. Maryško, P. Veverka, E. Pollert, J. Magn. Magn. Mater. 302 (2006) 315–320.
[16] G.F. Goya, T.S. BerquÓ, F.C. Fonseca, M.P. Morales, J. Appl. Phys. 94 (2003) 3520–3529.
[17] J. Nogués, V. Skumryev, J. Sort, S. Stoyanov, D. Givord, Phys. Rev. Lett. 97 (2006) 157203–157207.
[18] Q.A. Pankhurst, J. Connolly, S.K. Jones, J. Dobson, J. Phys. D: Appl. Phys. 36 (2003) R167–R181.
[19] J.L. Dormann, D. Fiorani, E. Tronc, Adv. Chem. Phys. 98 (1997) 283–494.